

Information scrambling in a partially confined quantum link model

Yifan Luo(罗祎帆), Zheng Tang(唐正), Li Chen(陈立), and Wei Zheng(郑炜)
Citation: Chin. Phys. B, 2025, 34 (**11**): 110301. DOI: 10.1088/1674-1056/ae00b1
http://cpb.iphy.ac.cn; http://iopscience.iop.org/cpb

What follows is a list of articles you may be interested in

Bayesian phase difference estimation based on single-photon projective measurement

Xu-Hao Yu(余旭豪), Ying Wei(韦颖), Ran Yang(杨然), Wen-Hui Song(宋文慧), Yingning Miao(缪应宁), Wei Zhou(周唯), Xinhui Li(李新慧), Xiaoqin Gao(高小钦), Yan-Xiao Gong(龚彦晓), and Shi-Ning Zhu(祝世宁)
Chin. Phys. B, 2025, 34 (**7**): 070305. DOI: 10.1088/1674-1056/adde33

Progressive quantum algorithm for maximum independent set with quantum alternating operator ansatz

Xiao-Hui Ni(倪晓慧), Ling-Xiao Li(李凌霄), Yan-Qi Song(宋燕琪), Zheng-Ping Jin(金正平), Su-Juan Qin(秦素娟), and Fei Gao(高飞)
Chin. Phys. B, 2025, 34 (**7**): 070304. DOI: 10.1088/1674-1056/addd83

Distributed quantum circuit partitioning and optimization based on combined spectral clustering and search tree strategies

Zilu Chen(陈子禄), Zhijin Guan(管致锦), Shuxian Zhao(赵书娴), and Xueyun Cheng(程学云)
Chin. Phys. B, 2025, 34 (**5**): 050305. DOI: 10.1088/1674-1056/adbada

Floquet engineering of a dynamical Z_2 lattice gauge field with ultracold atoms

Xiangxiang Sun(孙祥祥), Hao-Yue Qi(齐浩月), Pengfei Zhang(张鹏飞), and Wei Zheng(郑炜)
Chin. Phys. B, 2024, 33 (**11**): 110304. DOI: 10.1088/1674-1056/ad7576

Selected topics of quantum computing for nuclear physics

Dan-Bo Zhang(张旦波), Hongxi Xing(邢宏喜), Hui Yan(颜辉), Enke Wang(王恩科), and Shi-Liang Zhu(朱诗亮)
Chin. Phys. B, 2021, 30 (**2**): 020306. DOI: 10.1088/1674-1056/abd761

RAPID COMMUNICATION

Information scrambling in a partially confined quantum link model

Yifan Luo(罗祎帆)[1,2], Zheng Tang(唐正)[3], Li Chen(陈立)[3,†], and Wei Zheng(郑炜)[1,2,4,‡]

[1] *Hefei National Laboratory for Physical Sciences at the Microscale and Department of Modern Physics, University of Science and Technology of China, Hefei* 230026, *China*

[2] *CAS Center for Excellence in Quantum Information and Quantum Physics, University of Science and Technology of China, Hefei* 230026, *China*

[3] *Institute of Theoretical Physics, State Key Laboratory of Quantum Optics and Quantum Optics Devices, Shanxi University, Taiyuan* 030006, *China*

[4] *Hefei National Laboratory, University of Science and Technology of China, Hefei* 230088, *China*

(Received 13 July 2025; revised manuscript received 27 August 2025; accepted manuscript online 29 August 2025)

Quantum link models (QLMs) serve as experimentally accessible platforms for studying lattice gauge theories with finite-dimensional Hilbert spaces. In this work, we investigate information scrambling in the partially confined phase of a spin-1 quantum link model by calculating the dynamics of out-of-time-ordered correlators (OTOCs) and entanglement entropy. We observe that, in the partially confined phase, information scrambling exhibits significant asymmetry, manifested as the unidirectional propagation of both OTOCs and entanglement entropy. This phenomenon stands in stark contrast to the isotropic spreading observed in the deconfined phase and the localization characteristic of the confined phase. Furthermore, the simultaneous occurrence of the unidirectional propagation of both OTOCs and entanglement entropy, together with the θ-induced asymmetric excitation propagation, reveals a direct connection between information scrambling and charge confinement.

Keywords: lattice gauge field, partial confinement phase, quantum link model

PACS: 03.67.Ac, 11.15.Ha

DOI: 10.1088/1674-1056/ae00b1 **CSTR:** 32038.14.CPB.ae00b1

1. Introduction

Information scrambling refers to the rapid spreading of initially localized information across an entire quantum system, leading to the generation of global entanglement and complex patterns of correlations.[1–3] This phenomenon is central to understanding the non-equilibrium dynamics of quantum many-body systems and has profound implications across various fields, including quantum thermalization,[4] quantum chaos,[5,6] and black-hole physics.[7] In thermalizing systems, quantum information initially encoded in local degrees of freedom rapidly disperses throughout the system via entanglement growth, leading to equilibration described by Gibbs statistical mechanics. Conversely, many-body localized (MBL) systems defy thermalization due to strong disorder and interactions, preserving local information over long times.[8] MBL phases exhibit quantum memory effects and non-ergodic behavior, indicating a breakdown of the eigenstate thermalization hypothesis (ETH), which manifests as a slow, logarithmic growth of entanglement.[9]

Confinement, a fundamental phenomenon in quantum chromodynamics (QCD),[10–12] prevents the isolation of quarks due to an interquark potential that grows with distance, thereby binding them into hadrons. A closely analogous mechanism of charge confinement exists in strongly coupled quantum electrodynamics (QED).[13,14] A paradigmatic example is the $(1+1)$-dimensional Schwinger model, where the effective coupling scales linearly with separation, rendering charge confinement the dominant regime. Recent advances in quantum simulation platforms — including ultracold atoms in optical lattices, trapped ions, and superconducting qubits — have enabled the experimental realization of synthetic gauge fields.[15–23] On these simulators, a topological θ-angle-induced confinement–deconfinement transition in a spin-$1/2$ quantum link model, which represents one of the simplest U(1) lattice gauge theories, has been observed.[24] In addition, a partially confined phase has been predicted in a spin-1 quantum link model. However, few works have explored the relationship between information scrambling and charge confinement properties.

In this work, we investigate information scrambling in the partially confined phase of a spin-1 quantum link model. To quantify information scrambling, we compute the time evolution of both the out-of-time-ordered correlator (OTOC) and the growth of entanglement entropy following a local perturbation. One key finding is that, in the partially confined phase, anisotropic information scrambling occurs: quantum entanglement rapidly develops on one side of the perturbation while remaining significantly suppressed on the opposite side. Furthermore, we calculate the charge dynamics after introducing

†Corresponding author. E-mail: lchen@sxu.edu.cn

‡Corresponding author. E-mail: zw8796@ustc.edu.cn

© 2025 Chinese Physical Society and IOP Publishing Ltd. All rights, including for text and data mining, AI training, and similar technologies, are reserved.

a gauge-violation perturbation and find that the unidirectional propagation of excitons perfectly synchronizes with asymmetric information spreading, revealing a direct connection between charge confinement properties and quantum information scrambling.

2. Model

The Hamiltonian of the one-dimensional quantum link model (QLM)[25–27] can be expressed as

$$\hat{H} = -J\sum_{j=1}^{N-1}\left(\frac{1}{\sqrt{2}}\hat{\psi}_j\hat{S}_j^{+}\hat{\psi}_{j+1}+\text{h.c.}\right) + m\sum_{j=1}^{N}\hat{\psi}_j^{\dagger}\hat{\psi}_j + g\sum_{j=1}^{N-1}\left[(-1)^j\hat{S}_j^z+h\right]^2. \tag{1}$$

In this formulation, $\hat{\psi}_j$ and $\hat{\psi}_j^{\dagger}$ represent the annihilation and creation operators of the fermionic matter field at site j, respectively. At odd-numbered sites, these fermions correspond to electrons, while at even-numbered sites, they represent positrons. The Pauli operators $\hat{S}_j^{\pm}$ describe the spin states on the links connecting adjacent matter sites j and $j+1$.

The Hamiltonian encompasses several distinct physical interactions. The off-diagonal first term describes the matter–gauge interaction between different states, coupling spin-flip processes with the creation and annihilation of particle pairs in the matter field. The second term represents the mass energy of the fermions in the matter field. The third term characterizes the electric field energy (where $g \geq 0$). The quantized electric field on the jth link is given by

$$\hat{E}_j = (-1)^j\hat{S}_j^z + h. \tag{2}$$

Here, $(-1)^j\hat{S}_j^z$ represents the electric field generated by the matter particles, with the alternating sign reflecting the opposite charges of electrons and positrons. The parameter h denotes an external background electric field.

A notable feature of this Hamiltonian is its U(1) local gauge symmetry. Under a local gauge transformation at any site j

$$\hat{G}_j(\phi)\hat{\psi}_j\hat{G}_j^{\dagger}(\phi) = \mathrm{e}^{-\mathrm{i}\phi}\hat{\psi}_j, \tag{3}$$

$$\hat{G}_j(\phi)\hat{S}_j^{+}\hat{G}_j^{\dagger}(\phi) = \mathrm{e}^{\mathrm{i}\phi}\hat{S}_j^{+}, \tag{4}$$

$$\hat{G}_j(\phi)\hat{S}_{j+1}^{+}\hat{G}_j^{\dagger}(\phi) = \mathrm{e}^{\mathrm{i}\phi}\hat{S}_{j+1}^{+}, \tag{5}$$

$$\hat{G}_j(\phi)\hat{S}_{j+1}^{z}\hat{G}_j^{\dagger}(\phi) = \hat{S}_{j+1}^{z}, \tag{6}$$

the Hamiltonian remains invariant, where the gauge transformation operator is defined as

$$\hat{G}_j(\phi) = \mathrm{e}^{\mathrm{i}\phi\hat{Q}_j}, \tag{7}$$

$$\hat{Q}_j = \hat{\psi}_j^{\dagger}\hat{\psi}_j + \hat{S}_j^z + \hat{S}_{j-1}^z. \tag{8}$$

$\hat{Q}_j$ is referred to as the gauge charge and serves as a locally conserved quantity in the Hamiltonian.

The U(1) local gauge symmetry divides the total Hilbert space into distinct gauge sectors, with each sector characterized by a unique set of gauge charges. The physical sector corresponds to the case where all gauge charges $\hat{Q}_j = 0$ for every site j. We define the charge density on the matter site as

$$\hat{\rho}_j = (-1)^j\hat{\psi}_j^{\dagger}\hat{\psi}_j. \tag{9}$$

This expression indicates that fermions on even (odd) sites carry negative (positive) charge. Equation (8) can then be rewritten as

$$\hat{E}_{j+1} - \hat{E}_j = \hat{\rho}_j, \tag{10}$$

which is nothing but Gauss's law on a one-dimensional lattice.

The properties of the artificial gauge field enable transitions between the physical sector and other sectors through specific operator actions, allowing exploration of the Hamiltonian's behavior in nonphysical sectors. A key example of this is the matter field operator, which does not preserve gauge invariance under local transformations, as evidenced by the nonzero commutation relation $[\hat{\psi}_j, \hat{Q}_j] \neq 0$. Quantum link models exhibit distinct characteristics depending on their spin representation. In this work, we focus on information scrambling in the spin-1 QLM. For comparison, we also present results for the spin-1/2 QLM, which display fundamentally different behaviors.

The topological angle θ,[14,28–30] a key parameter in these systems, takes the form $\theta = \pi + 2\pi h$ for the spin-1/2 QLM and $\theta = 2\pi h$ for the spin-1 QLM. In the spin-1/2 case, the system exhibits two distinct phases depending on θ: a confined phase when $\theta \neq \pi$, and a phase with global Z_2 translation symmetry when $\theta = \pi$. At $\theta = \pi$, the system undergoes a confinement–deconfinement transition at a critical mass $m^* \approx 1$.[31] These theoretical and numerical predictions have been experimentally validated using a Bose–Hubbard simulator.[24]

The spin-1 QLM exhibits partial confinement behavior at $\theta = \pi$.[32] Partial confinement, first identified by Coleman in 1976 in the context of the continuous Schwinger model,[14] represents an intermediate regime in which charge confinement depends on the relative positions of particles.

To demonstrate these properties, we analyze the partially confined phase with parameters $m = J$, $g = J$, and $\theta = \pi$, as shown in Fig. 1. By applying excitation operators $\hat{\psi}_j^{\dagger}\hat{S}_j^{-}\hat{\psi}_{j+1}^{\dagger}$ and $\hat{\psi}_{j+1}^{\dagger}\hat{S}_{j+1}^{-}\hat{\psi}_{j+2}^{\dagger}$ to the ground state, we observe distinct temporal evolution patterns that characterize this phase.

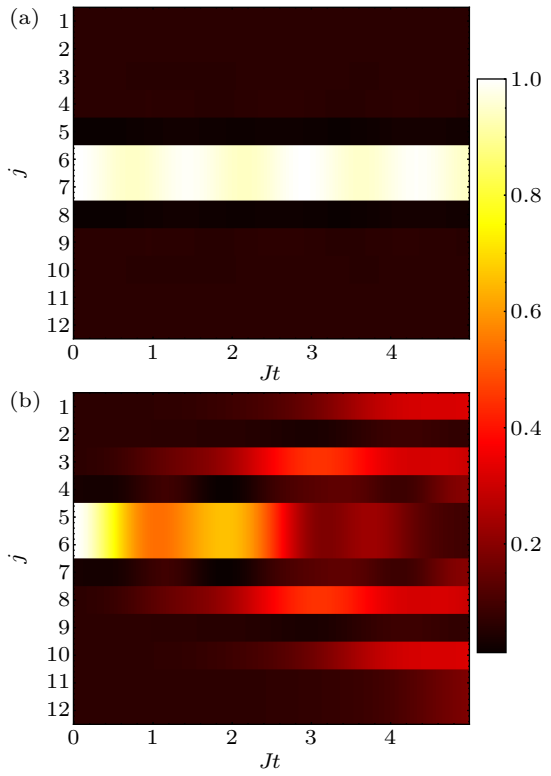


Fig. 1. Time evolution of the matter-site densities for $m = J$, $g = J$, and $\theta = \pi$ in a system of twelve matter sites. (a) The initial state is $\hat{\psi}_6^\dagger \hat{S}_6^- \hat{\psi}_7^\dagger |g\rangle$, representing the excitation of positive-negative charge pairs, which exhibit frozen dynamics, consistent with the confined phase. (b) The initial state is $\hat{\psi}_5^\dagger \hat{S}_5^- \hat{\psi}_6^\dagger |g\rangle$, representing the excitation of negative-positive charge pairs, with the extra physical charge delocalized, consistent with the deconfined phase.

3. Partial scrambling of information

To characterize the distinctive information dynamics in the partially confined phase of the spin-1 QLM, we examine two key quantum information metrics: the out-of-time-ordered correlator (OTOC) and the entanglement entropy. These measures provide insights into the partial scrambling behavior that is unique to this phase.

The OTOC is defined as

$$O(t) = \langle \hat{W}(t)^\dagger \hat{V}^\dagger \hat{W}(t) \hat{V} \rangle, \tag{11}$$

where $\hat{W}$ and $\hat{V}$ are arbitrary operators. Here, $\hat{W}(t) = e^{i\hat{H}t} \hat{W} e^{-i\hat{H}t}$ represents the time evolution of the operator $\hat{W}$ under the Hamiltonian $\hat{H}$, and the expectation value is taken with respect to the initial state $|\psi_0\rangle$. The OTOC provides a powerful framework for analyzing how local quantum information disperses in quantum many-body systems.

For our analysis, we consider a system comprising 12 gauge sites under open boundary conditions. In our calculations, we select the ground state of the physical sector, $|g\rangle$, as the initial state. Two specific operators are chosen to probe the system dynamics: the gauge-violating operator $\hat{V} = \hat{\psi}_6^\dagger$, which creates a matter excitation at site 6, and the gauge-invariant operator $\hat{W} = \hat{n}_l$, which measures the local particle number at site l, where l is an even number. The calculation workflow is presented in Fig. 2.

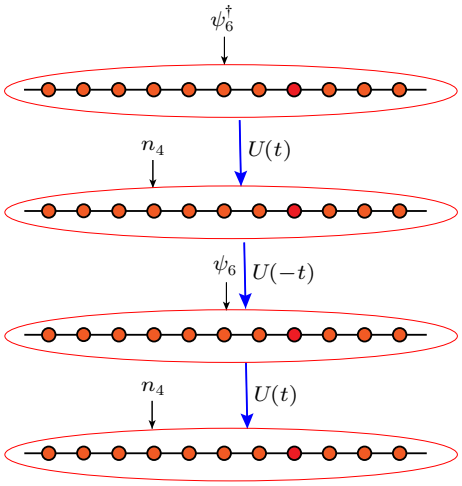


Fig. 2. Schematic illustration of the OTOC calculation procedure. The operator $\hat{W}$ is chosen as $\hat{\psi}_6^\dagger$, while the operator $\hat{V}$ is taken as $\hat{n}_4$.

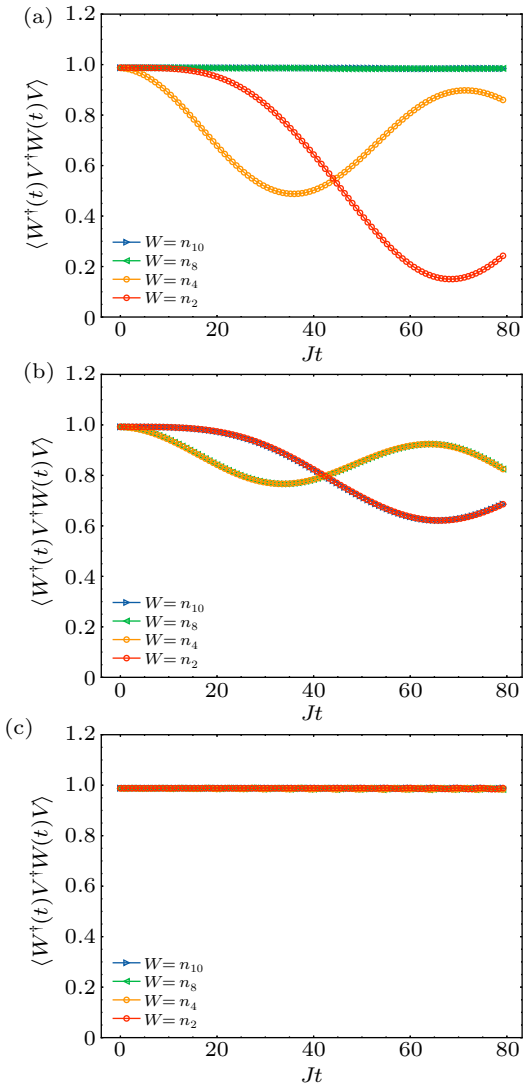


Fig. 3. Time evolution of the out-of-time-ordered correlator (OTOC) for different choices of the $\hat{W}$ operator in various phases. (a) Spin-1 QLM with $m = 4J$, $g = J$, and $\theta = \pi$ (partially confined phase). (b) Spin-1/2 QLM with $m = 4J$, $g = J$, and $\theta = \pi$ (deconfined phase). (c) Spin-1 QLM with $m = 4J$, $g = J$, and $\theta = 0$ (confined phase).

As shown in Fig. 3(a), the OTOC exhibits distinctly different dynamical behaviors depending on whether $l > 6$ or $l < 6$. For sites to the right of site 6, the OTOC decays rapidly over time, whereas for sites to the left of site 6, it remains nearly constant. This asymmetric behavior indicates that local information excited at the sixth matter site propagates exclusively leftward rather than isotropically, a phenomenon we refer to as partial information scrambling.

For comparison, Fig. 3(b) illustrates the OTOC evolution in the deconfined phase of the spin-1/2 quantum link model, characterized by isotropic information propagation, while Fig. 3(c) presents the OTOC evolution in the confined phase of the spin-1 quantum link model.

The partial scrambling of information can also be characterized by examining the dynamics of the entanglement entropy, defined as

$$S(\rho_{\mathrm{A}}) = -\mathrm{Tr}[\rho_{\mathrm{A}} \log(\rho_{\mathrm{A}})], \tag{12}$$

where ρ_{A} denotes the reduced density matrix of subsystem A, obtained by tracing out subsystem B: $\rho_{\mathrm{A}} = \mathrm{Tr}_{\mathrm{B}}(\rho_{\mathrm{AB}})$, with ρ_{AB} being the density matrix of the complete system. Within our chosen gauge, the quantum state can be expressed as a superposition of direct product spin states. We partition the spin chain into two subsystems by choosing a cutting point, such that the spins to the left of this point form subsystem A, while those to the right form subsystem B. A schematic representation of this partition is shown in Fig. 4.

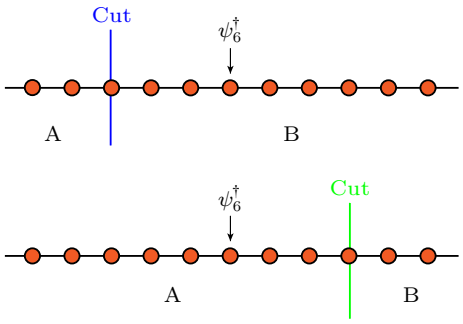


Fig. 4. Schematic illustration of entanglement entropy calculations for different partition cuts. In the upper panel, the blue line divides the system into subsystem A (comprising three spins on the left) and subsystem B (comprising the remaining spins on the right). The lower panel shows an alternative partitioning, where the green line separates nine spins (subsystem A) from the remainder of the system (subsystem B).

The entanglement entropy dynamics were investigated using the initial state $\hat{\psi}_6^\dagger|g\rangle$, following the same procedure as in the OTOC analysis. Our calculations reveal two distinct patterns in the time evolution of the entanglement entropy, depending on whether the bipartition point lies to the left or right of the sixth matter site, as illustrated in Fig. 5(a). For comparison, Fig. 5(b) shows the entanglement entropy evolution in the deconfined phase of the spin-1/2 quantum link model.

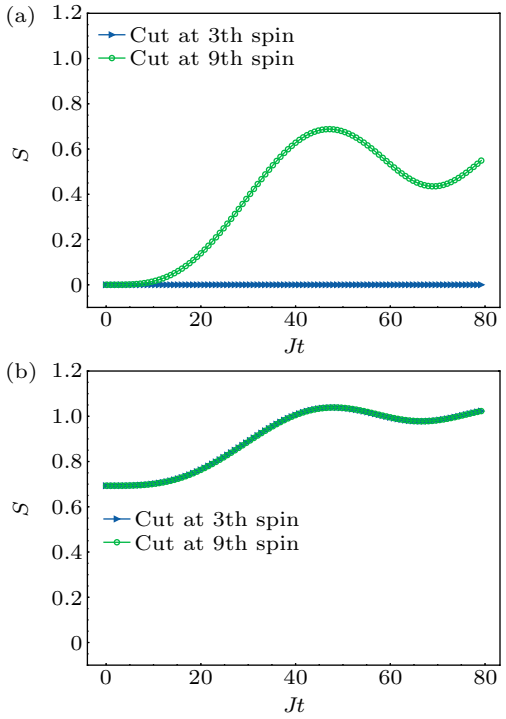


Fig. 5. Time evolution of the entanglement entropy for different bipartition points between subsystems A and B. (a) Spin-1 QLM with $m = 4J$, $g = J$, and $\theta = \pi$ (partially confined phase). (b) Spin-1/2 QLM with $m = 4J$, $g = J$, and $\theta = \pi$ (deconfined phase).

When the bipartition point is located to the right of the sixth matter site, the entanglement entropy between subsystems A and B remains nearly zero and exhibits minimal variation over time. This extremely low entanglement entropy indicates that quantum correlations between the subsystems are strongly suppressed, thereby restricting their capacity for information transfer. This observation further corroborates our finding that local information excited at the sixth matter site propagates exclusively leftward.

Notably, we find that this directional behavior reverses when the initial excitation is applied to an odd-numbered matter site, where information instead propagates solely to the right. These results collectively demonstrate the highly directional nature of information scrambling in the partially confined phase of the spin-1 quantum link model.

A notable distinction between the confined and deconfined phases can be identified through the correlation function $\langle g|\hat{\psi}_i(t)\hat{\psi}_i^\dagger(0)|g\rangle$ and its Fourier transform, commonly referred to as gauge-violation spectroscopy.[33] The confined phase exhibits a delta-function spectrum, whereas the deconfined phase displays a spectrum with finite width. However, this approach is insufficient to discriminate between the deconfined and partially confined phases, as their spectral features appear nearly identical.

In this context, the detection of partial information scrambling provides a more sensitive and conclusive diagnostic. The distinctly directional propagation patterns observed in the partially confined phase serve as a unique signature that differ-

entiates it from both the confined and deconfined regimes, offering a more comprehensive characterization of the system's quantum dynamical behavior.

4. Physical mechanism

To elucidate the underlying mechanism of partial information scrambling, we investigate the time evolution of the matter-site occupation numbers $\langle \hat{n} \rangle$, starting from the initial state $\hat{\psi}_6^\dagger |g\rangle$. While this method has previously been employed to distinguish between the confined and deconfined phases in the spin-1/2 quantum link model,[34] our extension to the spin-1 case reveals new physical insights, as illustrated in Fig. 6. The application of the gauge-violating operator drives the system into a non-physical sector, where the propagation of a single-particle excitation exhibits a pronounced directional asymmetry. This behavior stands in stark contrast to the spatially localized dynamics observed in the confined phase and the isotropic propagation characteristic of the deconfined regime.

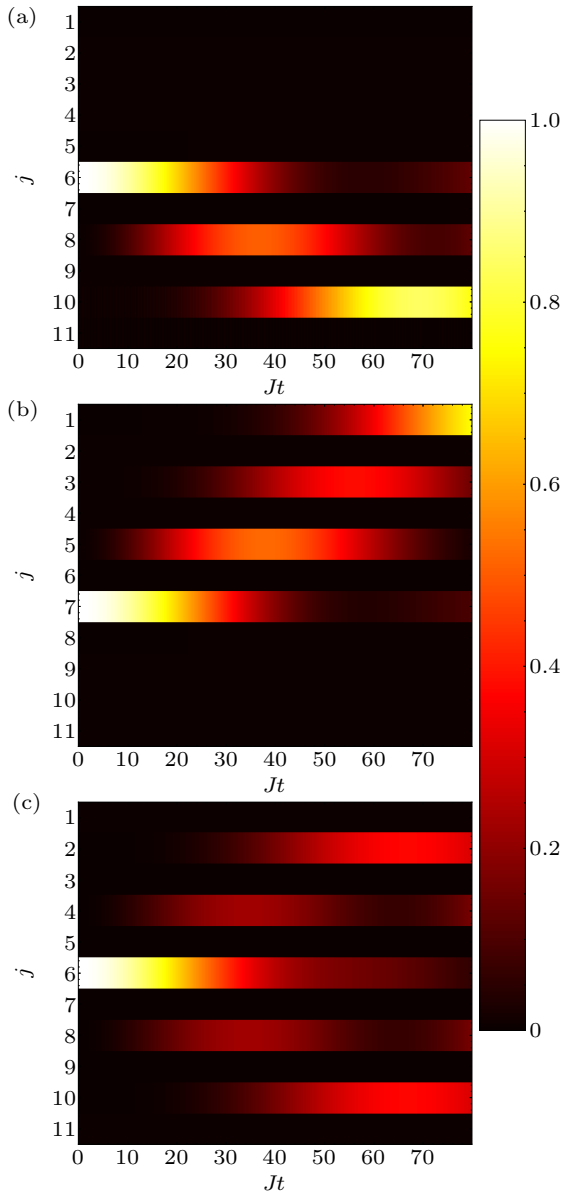


Fig. 6. Time evolution of the matter-site densities. (a) Spin-1 QLM with $m = 4J$, $g = J$, and $\theta = \pi$ (partially confined phase). The initial state is $\hat{\psi}_6^\dagger |g\rangle$. (b) Spin-1 QLM with $m = 4J$, $g = J$, and $\theta = \pi$ (partially confined phase). The initial state is $\hat{\psi}_7^\dagger |g\rangle$. (c) Spin-1/2 QLM with $m = 4J$, $g = J$, and $\theta = \pi$ (deconfined phase). The initial state is $\hat{\psi}_6^\dagger |g\rangle$.

Building upon our analysis of particle propagation, it is instructive to examine the fundamental distinctions between spin-1 and spin-1/2 quantum link models, which have been extensively explored in both theoretical and experimental studies.[25,31,34–40] A key difference lies in their topological characteristics: spin-1/2 models inherently possess a topological angle of $\theta = \pi$ (or $\theta = -\pi$) in the absence of external fields, whereas realizing this critical angle and inducing a phase transition in spin-1 models requires the application of an external electric field. The presence of such a field introduces a preferential direction for charge motion — positive charges drift along the field lines, while negative charges move oppositely. This directional bias in charge transport ultimately gives rise to the phenomenon of partial information scrambling.

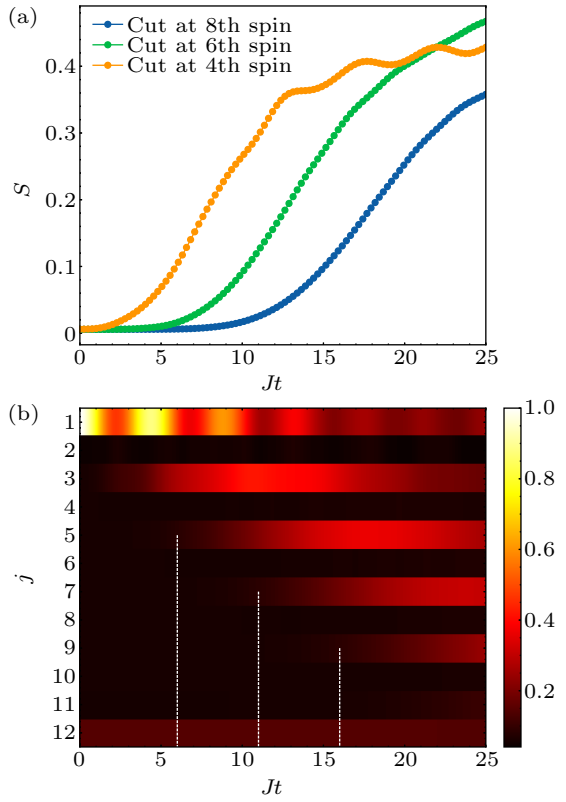


Fig. 7. Quasiparticle propagation and its relation to information scrambling for $m = J$, $g = J$, and $\theta = -\pi$. (a) Time evolution of the entanglement entropy for different bipartition points between subsystems A and B; the initial state is $\hat{\psi}_1^\dagger |g\rangle$. (b) Time evolution of the matter-site densities with the same initial state, $\hat{\psi}_1^\dagger |g\rangle$. White dashed lines indicate the times at which quasiparticles reach the corresponding matter sites.

To establish a direct connection between quasiparticle propagation and information scrambling, we simultaneously monitor the time evolution of entanglement entropy and matter-site occupation densities in the spin-1 quantum link

model, as illustrated in Fig. 7. Our results reveal a clear correlation: the entanglement entropy between subsystems A and B exhibits a rapid increase precisely when quasiparticles reach the interface separating these regions. This synchronization provides compelling evidence of the intrinsic link between particle transport and information spreading within the system.

5. Summary

In this work, we systematically investigated quantum information scrambling in the partially confined phase of a spin-1 quantum link model. Through numerical analysis of the OTOC and entanglement entropy dynamics, we demonstrated that information scrambling exhibits pronounced anisotropy in this regime: entanglement propagates exclusively to one side of the perturbation while remaining suppressed on the opposite side. This behavior contrasts sharply with the isotropic spreading observed in the deconfined phase and the frozen dynamics characteristic of the confined phase.

The observed directional scrambling arises from the interplay between the external electric field (encoded via θ) and the gauge structure of the spin-1 QLM, which promotes unidirectional quasiparticle propagation. Specifically, in the partially confined phase, the θ-angle modifies the effective potential between charges, enabling localized excitations to propagate asymmetrically. This mechanism is further corroborated by the occupation density dynamics of matter sites, where gauge-violating operators induce motion only along the direction of the electric field.

Our findings establish partial confinement as a distinct intermediate regime that governs quantum information dynamics, bridging conventional confinement and deconfinement paradigms. The directional scrambling mechanism provides a sensitive diagnostic tool for distinguishing phases in lattice gauge theories, complementing traditional correlation function analyses. Moreover, these results highlight the potential of quantum simulators to probe non-equilibrium phenomena in lattice gauge theories, with broader implications for understanding thermalization, many-body localization, and black-hole information dynamics.

Acknowledgments

This project was supported by the National Natural Science Foundation of China (Grant Nos. GG2030007011 and GG2030040453) and the Innovation Program for Quantum Science and Technology (Grant No. 2021ZD0302004). L.C. acknowledges support from the National Natural Science Foundation of China (Grant No. 12174236) and the fund for the Shanxi 1331 Project.

References

[1] Xu S and Swingle B 2024 *PRX Quantum* **5** 010201
[2] Swingle B 2018 *Nat. Phys.* **14** 988
[3] Li J, Fan R, Wang H, Ye B, Zeng B, Zhai H, Peng X and Du J 2017 *Phys. Rev. X* **7** 031011
[4] Nandkishore R and Huse D A 2015 *Annu. Rev. Condens. Matter Phys.* **6** 15
[5] Garcia-Mata I, Jalabert R A and Wisniacki D A 2023 *Scholarpedia* **18** 55237
[6] Hahn D, Luitz D J and Chalker J T 2024 *Phys. Rev. X* **14** 031029
[7] Maldacena J, Shenker S H and Stanford D 2016 *J. High Energy Phys.* **2016** 106
[8] Fan R, Zhang P, Shen H and Zhai H 2017 *Sci. Bull.* **62** 707
[9] Lerose A and Pappalardi S 2020 *Phys. Rev. Res.* **2** 012041
[10] Wilson K G 1974 *Phys. Rev. D* **10** 2445
[11] Allan C G, Dashen R and Gross D J 1977 *Phys. Lett. B* **66** 375
[12] Greensite J 2011 *An introduction to the confinement problem* (Springer) p. 821
[13] Schwinger J 1962 *Phys. Rev.* **125** 397
[14] Coleman S 1976 *Ann. Phys.* **101** 239
[15] Wiese U 2013 *Ann. Phys. (Leipzig)* **525** 777
[16] Bañuls M C, Blatt R, Catani J, *et al.* 2020 *Euro. Phys. J. D* **74** 165
[17] Chen L, Zhu F, Tang Z and Gao C 2023 *Emerg. Sci. Technol.* **2** 49
[18] Bauer C W, Davoudi Z, Balantekin A B, *et al.* 2023 *PRX Quantum* **4** 027001
[19] Aidelsburger M, Barbiero L, Bermudez A, *et al.* 2022 *Phil. Trans. R. Soc. A* **380** 20210064
[20] Halimeh J C and Hauke P 2020 *Phys. Rev. Lett.* **125** 030503
[21] Halimeh J C, Kasper V and Hauke P 2020 arXiv:2009.07848 [cond-mat.quant-gas]
[22] Bender J, Emonts P and Cirac J I 2023 *Phys. Rev. Res.* **5** 043128
[23] Klco N, Roggero A and Savage M J 2022 *Rep. Prog. Phys.* **85** 064301
[24] Zhang W Y, Liu Y, Cheng Y, He M G, Wang H Y, Wang T Y, Zhu Z X, Su G X, Zhou Z Y, Zheng Y G, Sun H, Yang B, Hauke P, Zheng W, Halimeh J C, Yuan Z S and Pan J W 2025 *Nat. Phys.* **21** 155
[25] Banerjee D, Dalmonte M, Müller M, Rico E, Stebler P, Wiese U J and Zoller P 2012 *Phys. Rev. Lett.* **109** 175302
[26] Chandrasekharan S and Wiese U J 1997 *Nucl. Phys. B* **492** 455
[27] Kühn S, Cirac J I and Bañuls M C 2014 *Phys. Rev. A* **90** 042305
[28] Jackiw R and Rebbi C 1976 *Phys. Rev. Lett.* **37** 172
[29] Batakis N and Lazarides G 1978 *Phys. Rev. D* **18** 4710
[30] Hooft G T 1976 *Phys. Rev. D* **14** 3432
[31] Halimeh J C, McCulloch I P, Yang B and Hauke P 2022 *PRX Quantum* **3** 040316
[32] Tang Z, Zhu F, Luo Y F, Zheng W and Chen L 2024 *Phys. Rev. A* **110** 033302
[33] Qi H Y and Zheng W 2024 *Phys. Rev. Res.* **6** 013047
[34] Cheng Y, Liu S, Zheng W, Zhang P and Zhai H 2022 *PRX Quantum* **3** 040317
[35] Surace F M, Mazza P P, Giudici G, Lerose A, Gambassi A and Dalmonte M 2020 *Phys. Rev. X* **10** 021041
[36] Mil A, Zache T V, Hegde A, Xia A, Bhatt R P, Oberthaler M K, Hauke K, Berges J and Jendrzejewski F 2020 *Science* **367** 1128
[37] Zhou Z Y, Su G X, Halimeh J C, Ott R, Sun H, Hauke P, Yang B, Yuan Z S, Berges J and Pan J W 2022 *Science* **377** 311
[38] Wang H Y, Zhang W Y, Yao Z, Liu Y, Zhu Z H, Zheng Y G, Wang X K, Zhai H, Yuan Z S and Pan J W 2023 *Phys. Rev. Lett.* **131** 050401
[39] Gao C, Liu J, Chang M, Pu H and Chen L 2022 *Phys. Rev. Res.* **4** L042018
[40] Gao C, Tang Z, Zhu F, Zhang Y, Pu H and Chen L 2023 *Phys. Rev. B* **107** 104302